

Modeling Relational Patterns for Logical Query Answering over Knowledge Graphs

Yunjie He and Mojtaba Nayyeri and Bo Xiong and Yuqicheng Zhu

University of Stuttgart

{yunjie.he, mojtaba.nayyeri, bo.xiong, yuqicheng.zhu}@ipvs.uni-stuttgart.de

Evgeny Kharlamov

Bosch Center for Artificial Intelligence

Evgeny.Kharlamov@de.bosch.com

Steffen Staab

University of Stuttgart and

University of Southampton

steffen.staab@ipvs.uni-stuttgart.de

Abstract

Answering first-order logical (FOL) queries over knowledge graphs (KG) remains a challenging task mainly due to KG incompleteness. Query embedding approaches this problem by computing the low-dimensional vector representations of entities, relations, and logical queries. KGs exhibit relational patterns such as symmetry and composition and modeling the patterns can further enhance the performance of query embedding models. However, the role of such patterns in answering FOL queries by query embedding models has not been yet studied in the literature. In this paper, we fill in this research gap and empower FOL queries reasoning with pattern inference by introducing an inductive bias that allows for learning relation patterns. To this end, we develop a novel query embedding method, RoConE, that defines query regions as geometric cones and algebraic query operators by rotations in complex space. RoConE combines the advantages of Cone as a well-specified geometric representation for query embedding, and also the rotation operator as a powerful algebraic operation for pattern inference. Our experimental results on several benchmark datasets confirm the advantage of relational patterns for enhancing logical query answering task.

1 Introduction

Answering first-order logical (FOL) queries over knowledge graphs (KGs) has been an important and challenging problem (Ren and Leskovec, 2020). Among various approaches, logical query embedding (Hamilton et al., 2018; Ren et al., 2020; Zhang et al., 2021; Ren and Leskovec, 2020) has received huge attention due to its great efficiency and effectiveness. Logical query embeddings take as input the KGs and a set of first-order logical queries that include existential quantification (\exists), conjunction (\wedge), disjunction (\vee), and negation (\neg). Figure 1 shows a concrete FOL query example that corresponds to the natural language query “List the capi-

$$q = A_7, \exists V: \neg \text{locatedAt}(V, \text{Europe}) \wedge (\text{held}(\text{WorldCup}, V) \vee \text{held}(\text{Olympics}, V)) \wedge \text{capitalOf}(A_7, V)$$

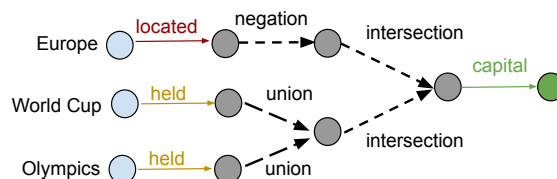


Figure 1: An example of FOL query corresponds to "List the capitals of non-European countries that have held either World Cup or Olympics".

tals of non-European countries that have held either World Cup or Olympics”. The methods model logic operations by neural operators that act in the vector space. In particular, they represent a set of entities as geometric shapes and design neural-network-based logical operators to compute the embedding of the logical queries. The similarity between the embedded logical query and a candidate answer is calculated to measure plausibility.

Relations in KGs may form particular patterns, e.g., some relations are symmetric (e.g., spouse) while others are anti-symmetric (e.g., parent_of); some relations are the inverse of other relations (e.g., son_of and father_of). Modeling relational patterns can potentially improve the generalization capability and has been extensively studied in link prediction tasks (Sun et al., 2019; Nayyeri et al., 2021). This has been shown particularly in Sun et al. (2019) where the RotatE model utilizes the rotation operation in Complex space to model relational patterns and enhance link prediction task. However, current logical query embedding models adopt deep neural logical operators and are not able to model relational patterns, which do matter for logical query answering. Figure 2 shows concrete examples of how relation patterns can impact complex query reasoning in KGs.

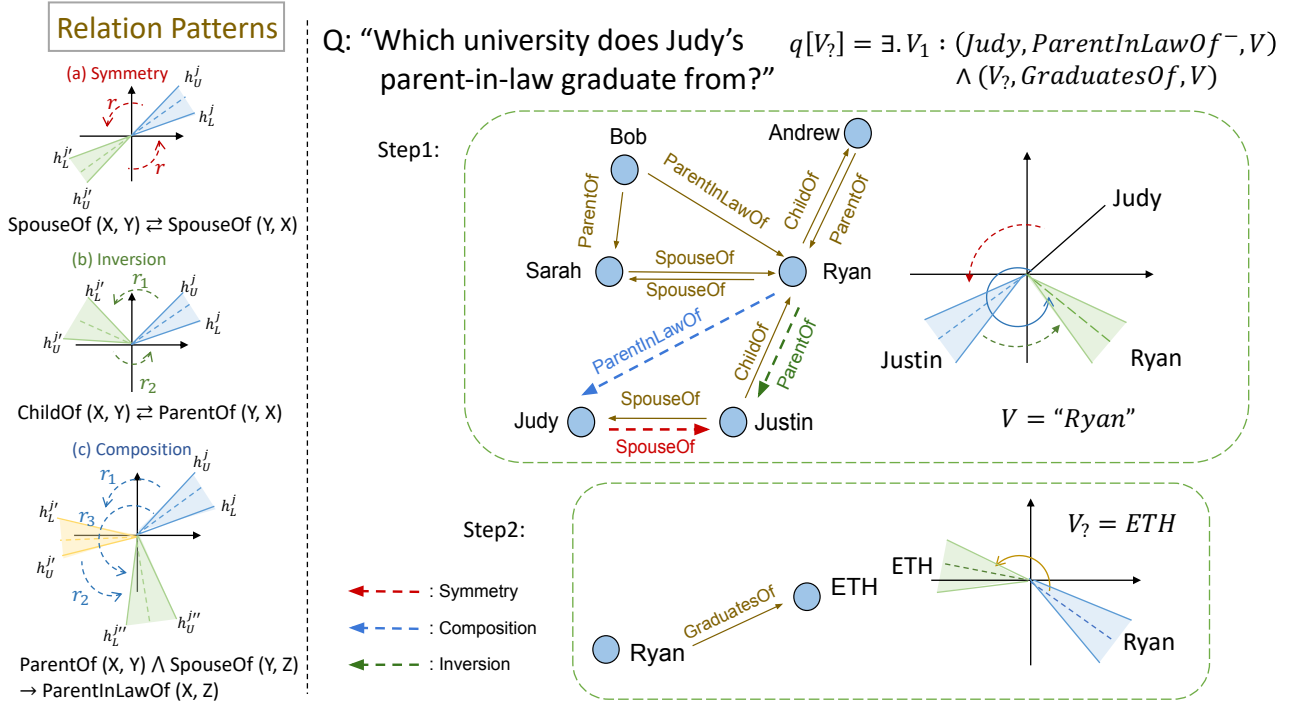


Figure 2: (top) An example showing how relation patterns influence query answering over incomplete KGs: the intermediate variable Judy’s father-in-law in the query cannot be directly extracted from the given facts; (bottom) An illustration of cone rotation. Based on the existing relations between Judy, Justin, and Ryan, and the learned potential relation patterns from other parts of the graph, the model is able to derive the following information by relational rotation: (i) Justin is Judy’s spouse (symmetric rotation) (ii) Justin is the child of Ryan (inversion rotation) (iii) Ryan is Judy’s father in law (compositional rotation). With the predicted query embedding on V , the model is able to derive where V graduated from by another relational rotation.

To model and infer various KG relational patterns in logical queries answering process, we propose a novel method called RoConE that combines the advantages of Cone as a well-specified geometric representation for query embedding (Zhang et al., 2021), and also the rotation operator (Sun et al., 2019) as a powerful algebraic operation for pattern inference. We define each relation as a rotation from the source entity set to the answer/intermediate entity set and perform neural logical operators upon the selected entity sets in the complex vector space. We provide theoretical proof of its ability to model relational patterns, as well as experimental results on how the relational patterns influence logical queries answering over three established benchmark datasets.

2 Related Work

To answer more complex queries, a number of path-based (Xiong et al., 2017a; Lin et al., 2018), neural (Hamilton et al., 2018; Ren et al., 2020; Kotnis et al., 2021), and neural-symbolic (Arakelyan et al., 2021; Zhu et al., 2022) methods have been devel-

oped. Among these methods, geometric and probabilistic query embedding approaches (Hamilton et al., 2018; Ren et al., 2020; Zhang et al., 2021; Ren and Leskovec, 2020) provide a way to tractably handle first-order logic operators in queries and equip excellent computing efficiency. This is done by representing entity sets as geometric objects or probability distributions, such as boxes (Ren et al., 2020), cones (Zhang et al., 2021), or Beta distribution (Ren and Leskovec, 2020), and performing neural logical operations directly on them. In this way, the expensive search for intermediate variables in multi-hop queries is avoided. All of the above query embedding methods commonly apply multi-layer perceptron networks for selecting answer entities of atomic queries by relation and performing logical operations. Thus, their ability to capture relation patterns in KGs remains unclear. Our proposed method RoConE fills in this gap and combines the benefits of both worlds (KG embedding and complex query answering) together.

3 Preliminaries

Knowledge Graph A KG $\mathcal{G} \subseteq \mathcal{E} \times \mathcal{R} \times \mathcal{E}$, where \mathcal{E} and \mathcal{R} represent the set of entities and relations respectively, can be defined as a set of subject-predicate-object $\langle s, p, o \rangle$ triples. For each triple $\langle e_i, r, e_j \rangle$, $e_{i,j} \in \mathcal{E}$ and $r \in \mathcal{R}$, it exists if and only if e_i is linked to e_j by relation r .

First-Order Logical Queries involving constants

First-Order Logical Queries are broad and here we consider answering a subset, i.e., multi-hop queries with constants and first-order logical operations including conjunction (\wedge), disjunction (\vee), existential quantification (\exists), and negation (\neg). The query consists of a set of constants (anchor entities) $\mathcal{E}_a \subset \mathcal{E}$, a set of existentially quantified bound variables V_1, \dots, V_m and a single target answer variable V_t . The disjunctive normal form of this subset of FOL queries is namely the disjunction of conjunctive formulas, and can be expressed as

$$q[V_t] = V_t. \exists V_1, \dots, V_m : c_1 \vee c_2 \vee \dots \vee c_n \quad (1)$$

where $c_i, i \in \{1, \dots, n\}$ corresponds to a conjunctive query with one or more atomic queries d i.e. $c_i = d_{i1} \wedge d_{i2} \wedge \dots \wedge d_{im}$. For each atomic formula, $d_{ij} = (e_a, r, V)$ or $\neg(e_a, r, V)$ or (V', r, V) or $\neg(V', r, V)$, where $e_a \in \mathcal{E}_a$, $V \in \{V_t, V_1, \dots, V_k\}$, $V' \in \{V_1, \dots, V_k\}$, $r \in \mathcal{R}$. The goal of logical query embedding is to find a set of answer entities $\{e_{t1}, e_{t2}, \dots\}$ for V_t , such that $q[V_t] = \text{True}$.

4 Methodology

To accommodate the learning of relation patterns in query answering over KGs, we propose a new model RoConE, which models entity sets as cones and relations as anti-clockwise angular rotations on cones in the complex plane. Each cone \mathbf{q} is parameterized by $\mathbf{q} = (\mathbf{h}_U, \mathbf{h}_L)$, where $|\mathbf{h}_{\{U,L\}}| = \mathbf{1}$, and $\mathbf{h}_U, \mathbf{h}_L \in \mathbb{C}^d$ represent the counter-clockwise upper and lower boundaries of a cone, such that

$$\begin{aligned} \mathbf{h}_U &\equiv e^{i\theta_U} \equiv e^{i(\theta_{ax} + \theta_{ap}/2)}, \\ \mathbf{h}_L &\equiv e^{i\theta_L} \equiv e^{i(\theta_{ax} - \theta_{ap}/2)}, \end{aligned} \quad (2)$$

where $\theta_{ax} \in [-\pi, \pi]^d$ represents the angle between the symmetry axis of the cone and $\theta_{ap} \in [0, 2\pi]^d$ represents the cone aperture, and d is the embedding dimension. The query and the set of entities are modeled as cones and each entity instance is modeled as a vector such that $\mathbf{h}_U = \mathbf{h}_L$.

4.1 Logical Operators

As illustrated in Figure 1, each logical query can be represented as a directed acyclic graph (DAG) tree, where the tree nodes correspond to constants/anchor node entities or variables, and the edges correspond to atom relations or logical operations in a query. Logical operations are performed along the DAG tree from constants to the target answer variable. Figure 3 visualizes these operations on 2D complex space. The logical operators can be defined as follows

Relational rotating projection Given a set of entities $\mathcal{S} \subset \mathcal{E}$ and a relation $r \in \mathcal{R}$, the projection operator selects the neighbouring entities $\mathcal{S}' \subset \mathcal{E}$ by relation such that $\mathcal{S}' = \{e \in \mathcal{S}, e' \in \mathcal{S}' : r(e, e') = \text{True}\}$. Existing query embedding methods (Zhang et al., 2021; Ren et al., 2020; Hamilton et al., 2018; Ren and Leskovec, 2020) apply multi-layer perceptron networks to accomplish this task. They do not accommodate the learning of potential KG relational patterns which might help in reasoning logical queries. Motivated by RotatE (Sun et al., 2019), we represent each relation \mathbf{r} as a counterclockwise relational rotation on query embeddings about the origin of the complex plane such that $\mathbf{r} = (\mathbf{r}_U, \mathbf{r}_L)$, where $|\mathbf{r}_{\{U,L\}}| = \mathbf{1}$, and $\mathbf{r}_U, \mathbf{r}_L \in \mathbb{C}^d$. Given the query embedding $\mathbf{q} = (\mathbf{h}_U, \mathbf{h}_L)$ and a relation \mathbf{r} , the selected query embedding $\mathbf{q}' = (\mathbf{h}'_U, \mathbf{h}'_L)$ is

$$\begin{aligned} \mathbf{h}'_U &= \mathbf{h}_U \circ \mathbf{r}_U \equiv e^{i(\theta_{ax} + \theta_{ax,r} + (\theta_{ap} + \theta_{ap,r})/2)}, \\ \mathbf{h}'_L &= \mathbf{h}_L \circ \mathbf{r}_L \equiv e^{i(\theta_{ax} + \theta_{ax,r} - (\theta_{ap} + \theta_{ap,r})/2)}, \end{aligned} \quad (3)$$

where \circ is the Hadamard (element-wise) product, and $\theta_{ax,r}, \theta_{ap,r}$ correspond to the equivalent relational rotation on θ_{ax}, θ_{ap} . Specifically, for each element of the cone embeddings, we have $h'_{U,i} = h_{U,i} r_{U,i}$ and $h'_{L,i} = h_{L,i} r_{L,i}$. Each element r_i of the relational rotation $\mathbf{r}_{\{U,L\}}$ corresponds to a counterclockwise rotation on the matching element of upper or lower boundaries by $\theta_{r,i}$ radians about the origin of the complex plane. By modeling the projection as relational rotation on a cone in the complex space, RoConE is shown to model and infer all three types of relation patterns introduced in Section 3. The lemmas and their proofs are in Appendix and the rotations corresponding to different relation patterns are visualized in Figure 4.

Intersection For the input cone embeddings of entity sets $\{\mathbf{q}_1, \dots, \mathbf{q}_n\}$, the intersection operator selects the intersection $\mathbf{q}' = \bigcap_{j=1}^n \mathbf{q}_j$

with the **SemanticAverage**¹(\cdot) and **CardMin**(\cdot) (Zhang et al., 2021), which calculate the semantic centers and apertures of cones respectively. Since we have each cone $\mathbf{q}_j = (\mathbf{h}_{j,U}, \mathbf{h}_{j,L}) \equiv (e^{i(\theta_{j,ax} + \theta_{j,ap}/2)}, e^{i(\theta_{j,ax} - \theta_{j,ap}/2)})$, the intersection $\mathbf{q}' = (\mathbf{h}'_U, \mathbf{h}'_L)$ can be defined as follows

$$\begin{aligned} \mathbf{h}'_U &= e^{i(\theta'_{ax} + \theta'_{ap}/2)}, \\ \mathbf{h}'_L &= e^{i(\theta'_{ax} - \theta'_{ap}/2)}, \end{aligned} \quad (4)$$

where

$$\begin{aligned} \theta'_{ax} &= \text{SemanticAverage}(\{(\theta_{j,ax}, \theta_{j,ap})\}_{j=1}^n), \\ \theta'_{ap} &= \text{CardMin}(\{(\theta_{j,ax}, \theta_{j,ap})\}_{j=1}^n). \end{aligned} \quad (5)$$

Disjunction Given the input cone embeddings of entity sets $\{\mathbf{q}_1, \dots, \mathbf{q}_n\}$ where $\mathbf{q}_j = (\mathbf{h}_{j,U}, \mathbf{h}_{j,L})$, the disjunction operator finds the union set $\mathbf{q} = \bigcup_{j=1}^n \mathbf{q}_j = \{\mathbf{q}_1, \dots, \mathbf{q}_n\}$, which is equivalent to

$$\{(\mathbf{h}_{1,U}^1, \mathbf{h}_{1,L}^1), \dots, (\mathbf{h}_{n,U}^1, \mathbf{h}_{n,L}^1)\}, \dots, \{(\mathbf{h}_{1,U}^d, \mathbf{h}_{1,L}^d), \dots, (\mathbf{h}_{n,U}^d, \mathbf{h}_{n,L}^d)\}$$

Following Ren et al. (2020), we also adopt DNF technique to translate FOL queries into the disjunction of conjunctive queries and only perform the disjunction operator in the last step in the computation graph.

Negation Given a set of entities $\mathcal{S} \subset \mathcal{E}$, the negation operator finds its complementary negation $\bar{\mathcal{S}} = \mathcal{E} \setminus \mathcal{S}$. Given the cone embedding of entity set \mathcal{S} , $\mathbf{q}^{\mathcal{S}} = (\mathbf{h}_U^{\mathcal{S}}, \mathbf{h}_L^{\mathcal{S}})$, its corresponding complementary negation $\bar{\mathbf{q}} = (\mathbf{h}_L^{\mathcal{S}}, \mathbf{h}_U^{\mathcal{S}})$.

4.2 Optimization

Given a set of training samples, our goal is to minimize the distance between the query cone embedding $\mathbf{q} = (\mathbf{h}_U^q, \mathbf{h}_L^q)$ and the answer entity vector \mathbf{h}^* while maximizing the distance between this query and negative samples. Thus, we define our training objective, the negative sample loss as

$$L = -\log\sigma(\gamma - d(\mathbf{h}^*, \mathbf{q})) - \frac{1}{k} \sum_{i=1}^k \log\sigma(d(\mathbf{h}_i^*, \mathbf{q}) - \gamma) \quad (6)$$

where $d(\cdot)$ is the combined distance specifically defined in Appendix C, γ is a margin, \mathbf{h}^* is a positive entity and \mathbf{h}_i^* is the i -th negative entity, k is the number of negative samples, and $\sigma(\cdot)$ represents the sigmoid function.

Dataset	Model	1p	2p	3p	2i	3i	pi	ip	2u	up
FB15k-237	GQE	35.2	7.4	5.5	23.6	35.7	16.7	10.9	8.4	5.8
	Query2Box	41.3	9.9	7.2	31.1	45.4	21.9	13.3	11.9	8.1
	BetaE	39.0	<u>10.9</u>	<u>10.0</u>	28.8	42.5	22.4	12.6	12.4	<u>9.7</u>
	ConE	41.8	12.8	11	<u>32.6</u>	47.3	25.5	14.0	14.5	10.8
	RoConE	42.2	10.5	7.5	33.5	48.1	<u>23.5</u>	14.5	<u>12.8</u>	8.9
NELL995	GQE	33.1	12.1	9.9	27.3	35.1	18.5	14.5	8.5	9.0
	Query2Box	42.7	14.5	11.7	34.7	45.8	23.2	17.4	12.0	10.7
	BetaE	53.0	13.0	11.4	37.6	47.5	24.1	14.3	12.2	8.5
	ConE	<u>53.1</u>	<u>16.1</u>	<u>13.9</u>	<u>40.0</u>	<u>50.8</u>	26.3	<u>17.5</u>	<u>15.3</u>	<u>11.3</u>
	RoConE	54.5	17.7	14.4	41.9	53.0	<u>26.1</u>	20.7	16.5	12.8

Table 1: MRR results (%) of RoConE, BETA E, Q2B, and GQE on answering EPFOL (\exists, \wedge, \vee) queries. The best statistic is highlighted in bold, while the second best is highlighted in underline.

5 Experiments

Experiment setup We evaluate RoConE on two benchmark datasets NELL995 (Xiong et al., 2017b) and FB15k-237 (Toutanova and Chen, 2015). RoConE is compared with various state-of-the-art query embedding models. Mean reciprocal rank (MRR) is used as the metric. More experimental details are in Appendix D.

Main results Table 1 summarizes the performance of all methods on answering various query types without negation. RoConE outperforms baseline methods on the majority of query types while achieving competitive results on the others. We also observed that RoConE shows better performances on NELL-995 than those on FB15k-237. We conjecture that this is due to the discrepancy in the distribution of relation patterns between these two datasets. As Table 2 shows, RoConE does not bring many improvements for answering query types involving negation. There are two folds of possible reasons that might lead to this result. Firstly, the traditional modeling of negation as complements may be problematic, which can be reflected in the poor performance of all existing QE models. This largely brings too much uncertainty into the query embedding and leads to severe bias in prediction. Secondly, the influence of relation patterns on negation queries is limited when we model negation as complements.

Ablation study To investigate the influence of relation patterns on the query answering model, we designed an ablation study for RoConE on NELL995. The results are reported in Table 3. RoConE (Base) denotes the neural baseline model without the relational rotating projection module. RoConE (S.E) and RoConE (Trunc) correspond

¹**SemanticAverage** and **CardMin** are explained in Appendix B

Dataset	Model	2in	3in	inp	pin	pni
FB15k-237	BetaE	5.1	7.9	7.4	3.6	3.4
	ConE	5.4	8.6	7.8	4.0	3.6
	RoConE	4.1	7.9	6.9	3.1	2.8
NELL995	BetaE	5.1	7.8	10	3.1	3.5
	ConE	5.7	8.1	10.8	3.5	3.9
	RoConE	5.2	7.7	9.4	3.2	3.7

Table 2: MRR results (%) of RoConE, BETAE, and ConE on answering queries with negation (−).

to two variants of RoConE with different rotation strategies. More details are elaborated in Appendix D.4. The overperformance of RoConE and RoConE (truncation) reconfirms the efficiency of relation patterns in logical query reasoning tasks.

Model	1p	2p	3p	2i	3i	pi	ip	2u	up
RoConE (Base)	53.1	16.1	13.9	40	50.8	26.3	17.5	15.3	11.3
RoConE (S.E.)	51.3	16.6	13.8	38.4	48.4	18.9	19.5	14.7	12.1
RoConE (Trunc)	53.7	17.8	14.2	41.9	53.0	27.5	20.4	16.6	12.7
RoConE	54.5	17.7	14.4	41.9	53.0	26.1	20.7	16.5	12.8

Table 3: Ablation study of RoConE on NELL995

6 Conclusion

In this paper, we theoretically and experimentally investigate the influence of relation patterns on enhancing the logical query reasoning task. By combining the relational rotating projection with the cone query embedding model in complex space, we improve FOL queries reasoning with relation pattern inference.

7 Limitations

RoConE incorporates the learning of potential KG relation patterns into the existing query embedding model for solving logical queries. We provide initial proof of the efficiency of relation patterns to complex reasoning via both theoretical explanations and experiments. One limitation of RoConE is that the relational rotating projection can not be generalized to other geometric query embedding methods, except for cone embedding, due to the restriction of natural geometry properties. For future work, we will propose more general and effective strategies to enhance the learning of relation patterns in the complex query reasoning task.

8 Ethics Statement

The authors declare that we have no conflicts of interest. This article does not contain any studies involving business data and personal information.

References

- Erik Arakelyan, Daniel Daza, Pasquale Minervini, and Michael Cochez. 2021. [Complex query answering with neural link predictors](#). In *9th International Conference on Learning Representations, ICLR 2021, Virtual Event, Austria, May 3-7, 2021*. OpenReview.net.
- William L. Hamilton, Payal Bajaj, Marinka Zitnik, Dan Jurafsky, and Jure Leskovec. 2018. [Embedding logical queries on knowledge graphs](#). In *Advances in Neural Information Processing Systems 31: Annual Conference on Neural Information Processing Systems 2018, NeurIPS 2018, December 3-8, 2018, Montréal, Canada*, pages 2030–2041.
- Bhushan Kotnis, Carolin Lawrence, and Mathias Niepert. 2021. [Answering complex queries in knowledge graphs with bidirectional sequence encoders](#). *Proceedings of the AAAI Conference on Artificial Intelligence*, 35(6):4968–4977.
- Xi Victoria Lin, Richard Socher, and Caiming Xiong. 2018. [Multi-hop knowledge graph reasoning with reward shaping](#). In *Proceedings of the 2018 Conference on Empirical Methods in Natural Language Processing*, pages 3243–3253, Brussels, Belgium. Association for Computational Linguistics.
- Mojtaba Nayyeri, Chengjin Xu, Yadollah Yaghoobzadeh, Sahar Vahdati, Mirza Mohtashim Alam, Hamed Shariat Yazdi, and Jens Lehmann. 2021. Loss-aware pattern inference: A correction on the wrongly claimed limitations of embedding models. In *Pacific-Asia Conference on Knowledge Discovery and Data Mining*, pages 77–89. Springer.
- Adam Paszke, Sam Gross, Francisco Massa, Adam Lerer, James Bradbury, Gregory Chanan, Trevor Killeen, Zeming Lin, Natalia Gimelshein, Luca Antiga, Alban Desmaison, Andreas Köpf, Edward Z. Yang, Zach DeVito, Martin Raison, Alykhan Tejani, Sasank Chilamkurthy, Benoit Steiner, Lu Fang, Junjie Bai, and Soumith Chintala. 2019. [Pytorch: An imperative style, high-performance deep learning library](#). *CoRR*, abs/1912.01703.
- Hongyu Ren, Weihua Hu, and Jure Leskovec. 2020. [Query2box: Reasoning over knowledge graphs in vector space using box embeddings](#). In *8th International Conference on Learning Representations, ICLR 2020, Addis Ababa, Ethiopia, April 26-30, 2020*. OpenReview.net.
- Hongyu Ren and Jure Leskovec. 2020. [Beta embeddings for multi-hop logical reasoning in knowledge graphs](#). In *Advances in Neural Information Processing Systems 33: Annual Conference on Neural Information Processing Systems 2020, NeurIPS 2020, December 6-12, 2020, virtual*.
- Zhiqing Sun, Zhi-Hong Deng, Jian-Yun Nie, and Jian Tang. 2019. [Rotate: Knowledge graph embedding by relational rotation in complex space](#). *CoRR*, abs/1902.10197.

Kristina Toutanova and Danqi Chen. 2015. [Observed versus latent features for knowledge base and text inference](#). In *Proceedings of the 3rd Workshop on Continuous Vector Space Models and their Compositionality*, pages 57–66, Beijing, China. Association for Computational Linguistics.

Wenhan Xiong, Thien Hoang, and William Yang Wang. 2017a. [DeepPath: A reinforcement learning method for knowledge graph reasoning](#). In *Proceedings of the 2017 Conference on Empirical Methods in Natural Language Processing*, pages 564–573, Copenhagen, Denmark. Association for Computational Linguistics.

Wenhan Xiong, Thien Hoang, and William Yang Wang. 2017b. [DeepPath: A reinforcement learning method for knowledge graph reasoning](#). In *Proceedings of the 2017 Conference on Empirical Methods in Natural Language Processing*, pages 564–573, Copenhagen, Denmark. Association for Computational Linguistics.

Manzil Zaheer, Satwik Kottur, Siamak Ravanbakhsh, Barnabas Poczos, Ruslan Salakhutdinov, and Alexander Smola. 2017. [Deep sets](#).

Zhanqiu Zhang, Jie Wang, Jiajun Chen, Shuiwang Ji, and Feng Wu. 2021. [Cone: Cone embeddings for multi-hop reasoning over knowledge graphs](#). In *Advances in Neural Information Processing Systems 34: Annual Conference on Neural Information Processing Systems 2021, NeurIPS 2021, December 6-14, 2021, virtual*, pages 19172–19183.

Zhaocheng Zhu, Mikhail Galkin, Zuobai Zhang, and Jian Tang. 2022. [Neural-symbolic models for logical queries on knowledge graphs](#). In *International Conference on Machine Learning, ICML 2022, 17-23 July 2022, Baltimore, Maryland, USA*, volume 162 of *Proceedings of Machine Learning Research*, pages 27454–27478. PMLR.

Appendices

A Lemmas and Corresponding Proofs

Lemma 1. *RoConE can infer the symmetry and anti-symmetry patterns.*

Proof. Given cone query embeddings $X = (\mathbf{h}_U^x, \mathbf{h}_L^x)$, $Y = (\mathbf{h}_U^y, \mathbf{h}_L^y)$ and relation $r = (\mathbf{r}_U, \mathbf{r}_L)$, if (X, r, Y) and (Y, r, X) hold, we have:

$$\begin{aligned} (\mathbf{h}_U^x \circ \mathbf{r}_U, \mathbf{h}_L^x \circ \mathbf{r}_L) &= (\mathbf{h}_U^y, \mathbf{h}_L^y), \\ (\mathbf{h}_U^y \circ \mathbf{r}_U, \mathbf{h}_L^y \circ \mathbf{r}_L) &= (\mathbf{h}_U^x, \mathbf{h}_L^x), \end{aligned} \quad (7)$$

$$\rightarrow (\mathbf{h}_U^y \circ \mathbf{r}_U \circ \mathbf{r}_U, \mathbf{h}_L^y \circ \mathbf{r}_L \circ \mathbf{r}_L) = (\mathbf{h}_U^y, \mathbf{h}_L^y)$$

thus, it is inferrable that X is symmetric to Y if and only if $(\mathbf{r}_U \circ \mathbf{r}_U = \mathbf{1}, \mathbf{r}_L \circ \mathbf{r}_L = \mathbf{1})$.

Similarly, if (X, r, Y) and $\neg(Y, r, X)$ hold, we have:

$$\begin{aligned} (\mathbf{h}_U^x \circ \mathbf{r}_U, \mathbf{h}_L^x \circ \mathbf{r}_L) &= (\mathbf{h}_U^y, \mathbf{h}_L^y), \\ (\mathbf{h}_U^y \circ \mathbf{r}_U, \mathbf{h}_L^y \circ \mathbf{r}_L) &\neq (\mathbf{h}_U^x, \mathbf{h}_L^x), \end{aligned} \quad (8)$$

$$\rightarrow (\mathbf{h}_U^x \circ \mathbf{r}_U \circ \mathbf{r}_U, \mathbf{h}_L^x \circ \mathbf{r}_L \circ \mathbf{r}_L) \neq (\mathbf{h}_U^x, \mathbf{h}_L^x)$$

thus, it is inferrable that X is anti-symmetric to Y if and only if $(\mathbf{r}_U \circ \mathbf{r}_U \neq \mathbf{1}, \mathbf{r}_L \circ \mathbf{r}_L \neq \mathbf{1})$. \square

Lemma 2. *RoConE can infer the inversion pattern.*

Proof. Given cone query embeddings $X = (\mathbf{h}_U^x, \mathbf{h}_L^x)$, $Y = (\mathbf{h}_U^y, \mathbf{h}_L^y)$ and relations $r_1 = (\mathbf{r}_{U,1}, \mathbf{r}_{L,1})$, $r_2 = (\mathbf{r}_{U,2}, \mathbf{r}_{L,2})$ if (X, r_1, Y) and (Y, r_2, X) hold, we have:

$$\begin{aligned} (\mathbf{h}_U^x \circ \mathbf{r}_{U,1}, \mathbf{h}_L^x \circ \mathbf{r}_{L,1}) &= (\mathbf{h}_U^y, \mathbf{h}_L^y), \\ (\mathbf{h}_U^y \circ \mathbf{r}_{U,2}, \mathbf{h}_L^y \circ \mathbf{r}_{L,2}) &= (\mathbf{h}_U^x, \mathbf{h}_L^x), \end{aligned} \quad (9)$$

$$\rightarrow (\mathbf{h}_U^y \circ \mathbf{r}_{U,2} \circ \mathbf{r}_{U,1}, \mathbf{h}_L^y \circ \mathbf{r}_{L,2} \circ \mathbf{r}_{L,1}) = (\mathbf{h}_U^y, \mathbf{h}_L^y)$$

thus, it is inferrable that X is inversible to Y if and only if $\mathbf{r}_{U,2} \circ \mathbf{r}_{U,1} = \mathbf{1}$ and $\mathbf{r}_{L,2} \circ \mathbf{r}_{L,1} = \mathbf{1}$. \square

Lemma 3. *RoConE can infer the composition pattern.*

Proof. Given cone query embeddings $X = (\mathbf{h}_U^x, \mathbf{h}_L^x)$, $Y = (\mathbf{h}_U^y, \mathbf{h}_L^y)$, $Z = (\mathbf{h}_U^z, \mathbf{h}_L^z)$ and relations $r_1 = (\mathbf{r}_{U,1}, \mathbf{r}_{L,1})$, $r_2 = (\mathbf{r}_{U,2}, \mathbf{r}_{L,2})$ if (X, r_1, Y) and (Y, r_2, Z) hold, we have:

$$\begin{aligned} (\mathbf{h}_U^x \circ \mathbf{r}_{U,1}, \mathbf{h}_L^x \circ \mathbf{r}_{L,1}) &= (\mathbf{h}_U^y, \mathbf{h}_L^y), \\ (\mathbf{h}_U^y \circ \mathbf{r}_{U,2}, \mathbf{h}_L^y \circ \mathbf{r}_{L,2}) &= (\mathbf{h}_U^z, \mathbf{h}_L^z), \\ (\mathbf{h}_U^x \circ \mathbf{r}_{U,3}, \mathbf{h}_L^x \circ \mathbf{r}_{L,3}) &= (\mathbf{h}_U^z, \mathbf{h}_L^z), \end{aligned} \quad (10)$$

\rightarrow

$$(\mathbf{h}_U^x \circ \mathbf{r}_{U,1} \circ \mathbf{r}_{U,2}, \mathbf{h}_L^x \circ \mathbf{r}_{L,1} \circ \mathbf{r}_{L,2}) = (\mathbf{h}_U^x \circ \mathbf{r}_{U,3}, \mathbf{h}_L^x \circ \mathbf{r}_{L,3})$$

thus, it is inferrable that relation r_3 is compositional of r_1 and r_2 if and only if $\mathbf{r}_{U,1} \circ \mathbf{r}_{U,2} = \mathbf{r}_{U,3}$. \square

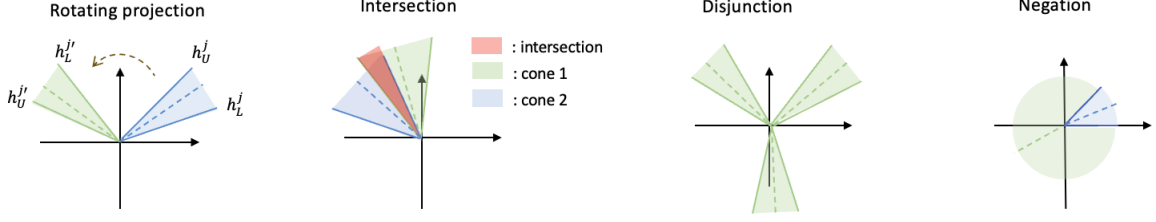


Figure 3: Visualization of logical operators (Zhang et al., 2021)

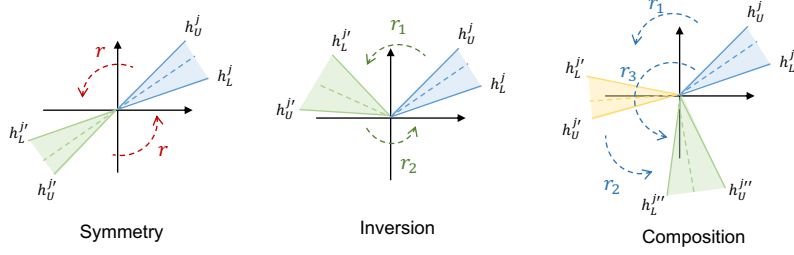


Figure 4: Relational rotations corresponding to different relation patterns on 2D complex plane.

B Details of Intersection Operator

In this section, we explain the details of two important components of the intersection operator, **SemanticAverage**(\cdot) and **CardMin**(\cdot)

SemanticAverage(\cdot) is expected to compute the semantic center θ'_{ax} of the input $\{(\theta_{j,ax}, \theta_{j,ap})\}_{j=1}^n$. Specifically, the computation process is provided as:

$$\begin{aligned} [\mathbf{x}; \mathbf{y}] &= \sum_{i=1}^n [\mathbf{a}_j \circ \cos(\theta_{j,ax}); \mathbf{a}_j \circ \sin(\theta_{j,ax})], \\ \theta'_{ax} &= \mathbf{Arg}(\mathbf{x}, \mathbf{y}), \end{aligned} \quad (11)$$

where \cos and \sin represent element-wise cosine and sine functions. $\mathbf{Arg}(\cdot)$ computes the argument given \mathbf{x} and \mathbf{y} . $\mathbf{a}_j \in \mathbb{R}^d$ are attention weights such that

$$[\mathbf{a}_j]_k = \frac{\exp([\mathbf{MLP}(\theta_{j,ax} - \theta_{j,ap}/2; \theta_{j,ax} + \theta_{j,ap}/2)]_k)}{\sum_{m=1}^n \exp([\mathbf{MLP}(\theta_{m,ax} - \theta_{m,ap}/2; \theta_{m,ax} + \theta_{m,ap}/2)]_k)}, \quad (12)$$

where $\mathbf{MLP} : \mathbb{R}^{2d} \rightarrow \mathbb{R}^d$ is a multi-layer perceptron network, $[\cdot; \cdot]$ is the concatenation of two vectors.

CardMin(\cdot) predicts the aperture θ'_{ap} of the intersection set such that $[\theta'_{ap}]_i$ should be no larger than any $\theta_{j,ap}^i$, since the intersection set is the subset of all input entity sets.

$$[\theta'_{ap}]_i = \min\{\theta_{1,ap}^i, \dots, \theta_{n,ap}^i\} \cdot \sigma([\mathbf{DeepSets}(\{(\theta_{j,ax}, \theta_{j,ap})\}_{j=1}^n)]_i) \quad (13)$$

where $\mathbf{DeepSets}(\{(\theta_{j,ax}, \theta_{j,ap})\}_{j=1}^n)$ (Zaheer et al., 2017) is given by

$$\mathbf{MLP}(\frac{1}{n} \sum_{j=1}^n \mathbf{MLP}([\theta_{j,ax} - \theta_{j,ap}/2; \theta_{j,ax} + \theta_{j,ap}/2])).$$

C Distance Function

Inspired by Zhang et al. (2021); Ren et al. (2020), the distance between \mathbf{q} and \mathbf{h}^* is defined as a combination of inside and outside distances, $d_{com}(\mathbf{q}, \mathbf{h}^*) = d_o + \lambda d_i$:

$$\begin{aligned} d_o(\mathbf{q}, \mathbf{h}^*) &= \min\{\|\mathbf{h}_U^q - \mathbf{h}^*\|_1, \|\mathbf{h}_L^q - \mathbf{h}^*\|_1\}, \\ d_i(\mathbf{q}, \mathbf{h}^*) &= \min\{\|\mathbf{h}_{ax}^q - \mathbf{h}^*\|_1, \|\mathbf{h}_U^q - \mathbf{h}_{ax}^q\|_1\}, \end{aligned} \quad (14)$$

where $\|\cdot\|_1$ is the L_1 norm, \mathbf{h}_{ax}^q represents the cone center, and $\lambda \in (0, 1)$.

Note that d_{com} can only be used for measuring the distance between a single query embedding and an answer entity vector. Since we represent the disjunctive queries in Disjunctive Normal Form as a set of query embeddings $\{\mathbf{q}_1, \dots, \mathbf{q}_n\}$, the distance between the answer vector and such set of embeddings is the minimum distance between the vector and each of these sets:

$$d_{dis}(\mathbf{q}, \mathbf{h}^*) = \min\{d_{com}(\mathbf{q}_1, \mathbf{h}^*), \dots, d_{com}(\mathbf{q}_n, \mathbf{h}^*)\} \quad (15)$$

Thus, the overall distance function can be defined as:

$$d(\mathbf{q}, \mathbf{h}^*) = \begin{cases} d_{com}(\mathbf{q}, \mathbf{h}^*), & \text{query without disjunction} \\ d_{dis}(\mathbf{q}, \mathbf{h}^*), & \text{query with disjunction} \end{cases} \quad (16)$$

D More Details about Experiments

In this section, we elaborate more details about our experiments. The code is anonymously available at <https://anonymous.4open.science/r/RoConE-1C1E>.

D.1 Dataset and Query structures

RoConE is compared with various state-of-the-art query embedding models, including GQE (Hamilton et al., 2018), Query2Box (Ren et al., 2020), BetaE (Ren and Leskovec, 2020), and ConE (Zhang et al., 2021). For a fair comparison with existing query embedding models, we use the same query structures and datasets NELL995 (Xiong et al., 2017a) and FB15k-237, and the open-sourced framework created by (Ren and Leskovec, 2020) for logical query answering tasks. Table 4 summarizes the descriptive statistics about the benchmark datasets. Figure 5 illustrates all query structures used in our experiments.

D.2 Hyperparameters and Computational Resources

All of our experiments are implemented in Pytorch (Paszke et al., 2019) framework and run on four Nvidia A100 GPU cards. For hyperparameters search, we performed a grid search of learning rates in $\{5 \times 10^{-5}, 10^{-4}, 5 \times 10^{-4}\}$, the batch size in $\{256, 512, 1024\}$, the negative sample sizes in $\{128, 64\}$, the regularization coefficient λ in $\{0.02, 0.05, 0.08, 0.1\}$ and the margin γ in $\{20, 30, 40, 50\}$. The best hyperparameters are saved in Table 5.

D.3 Evaluation Metrics

In this paper, we use Mean Reciprocal Rank (MRR) as the evaluation metric. Given a sample of queries Q , Mean reciprocal rank represents the average of the reciprocal ranks of results:

$$MRR = \frac{1}{|Q|} \sum_{i=1}^{|Q|} \frac{1}{rank_i}$$

D.4 Variants of relational projection strategies

To better incorporate the learning the relation patterns in query embedding model, we proposed alternative two variants of the relational rotation projection strategy:

- RoConE (Trunc): after relational rotation, the two boundaries of query embedding are truncated to ensure that aperture will not be greater than π .

- RoConE (S.E): replaces relational rotation on boundaries by a non-linear sigmoid function which maps the boundaries to shrink or expand and only maintains rotations on θ_{ax} .

D.5 Error Bars of Main Results

We have run RoConE 10 times with different random seeds, and obtain mean values and standard deviations of RoConE’s MRR results on EPFO and negation queries. Table 6 shows that mean values and standard deviations of RoConE’s MRR results on EPFOL queries. Table 7 shows mean values and standard deviations of RoConE’s MRR results on negation queries.

Dataset	Training		Validation		Testing	
	EPFOL	Negation	1p	others	1p	others
FB15k-237	149,689	14,968	20,101	5,000	22,812	5,000
NELL995	107,982	10,798	16,927	4,000	17,034	4,000

Table 4: Statistics of benchmark datasets : FB15k-237 and NELL995. EPFOL represents queries without negation, namely 1p/2p/3p/2i/3i.

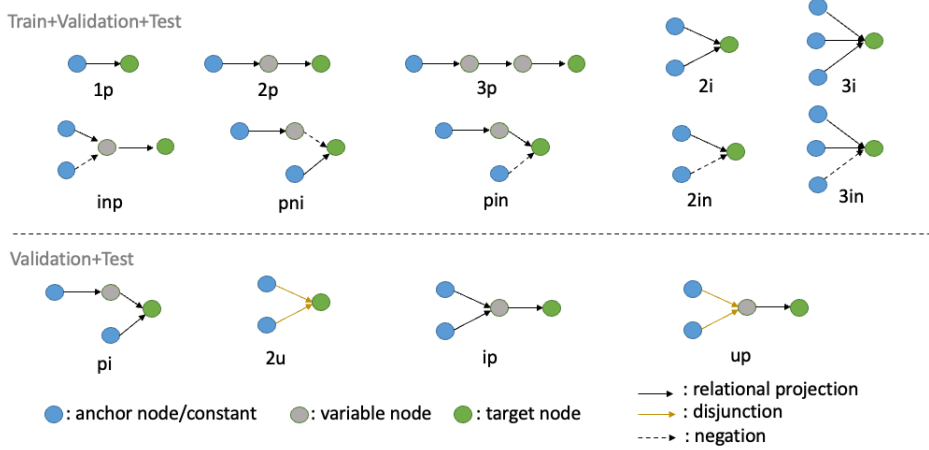


Figure 5: Fourteen types of queries used in the experiments. "p" represents relational projection, "i" represents intersection, "u" represents union and "n" represents negation. The upper of queries is used in the training stage, while all queries are evaluated in the validation and test stages.

Dataset	d	b	n	γ	l	λ
FB15k-237	1600	128	512	30	5×10^{-5}	0.1
NELL995	800	128	512	20	1×10^{-4}	0.02

Table 5: Hyperparameters found by grid search. d represents the embedding dimension, b is the batch size, n is the negative sampling size, γ is the margin in loss, l represents the learning rate, λ is the regularization parameter in the distance function.

Dataset	1p	2p	3p	2i	3i	pi	ip	2u	up
FB15k-237	42.2± 0.054	10.5± 0.108	7.5± 0.142	33.5± 0.075	48.1± 0.172	23.5± 0.105	14.5± 0.183	12.8± 0.096	8.9± 0.193
NELL995	54.5± 0.097	17.7± 0.152	14.4± 0.192	41.9± 0.130	53.0± 0.038	26.1± 0.084	20.7± 0.146	16.5± 0.112	12.8± 0.137

Table 6: RoConE's MRR mean values and standard variances (%) on answering EPFO (\exists , \wedge , \vee) queries

Dataset	2in	3in	inp	pin	pni
FB15k-237	4.1± 0.089	7.9± 0.092	6.9± 0.161	3.1± 0.083	2.8± 0.077
NELL995	5.2± 0.012	7.7± 0.079	9.4± 0.154	3.2± 0.012	3.7± 0.097

Table 7: RoConE's MRR mean values and standard variances (%) on answering negation queries